Bulg. J. Phys. **45** (2018) 247–254

Electronic Properties of Semiconductor Superlattices: Numerical Study of the Dimer Effect

M. Dairi[1], **A. Brezini**[1], **A. Zanoun**[2]
[1]Laboratoire LaMiN, Département Physique-Chimie, ENP Oran BP 1523 Oran El M'Naouer 31000 Oran, Algérie
[2]Département Physique-Chimie, ENP Oran BP 1523 Oran El M'Naouer 31000 Oran, Algérie

Received: *August 10, 2017*

Abstract. The dynamics of electrons in disordered semiconductor superlattices is investigated. A particular interest has been paid to the localization and delocalization behavior of electrons, in various situations including both ordered, disordered superlattices as well as the presence of random dimer. The random dimer effect is shown to have a direct effect on electronic and transport properties of the system. It is suggested a possible experimental observation of the Anderson localization. Typically, the over quoted GaAs/$Al_xGa_{1-x}As$ superlattice (SL) has been considered. Here the random dimer is introduced into the sample by means that two $Al_xGa_{1-x}As$ barriers of different Al mole fractions are introduced at random in the SL, with the restriction that one of them appear only in pairs. The present results can be checked experimentally. The main effect is the breakdown of localization and the existence of extended states having high properties of electronic transport. This feature may be conveniently used to develop a basis of new filter like or any other specific purpose electronic devices.

PACS codes: 71.23.An

1 Introduction

The recent advances in nanotechnology made it possible to grow artificial semiconductor superlattices (SL) with tailored physical properties and open the possibility to check experimentally the theoretical predictions (for a review see [1]).

Since the original work of Anderson [2], the electron localization phenomenon induced by disorder, is still alive and continue to be of great interest for physicists. Recently, several works performed subsequently suggested the possible suppression of localization in one-dimensional disordered systems, breaking down the so-called Mott and Twose theorem [3]. In particular, Diez et al. [4]

conjectured the suppression of localization in GaAs/$Al_xGa_{1-x}As$ SL with dimer wells located at random, referred to as DWSL. Such a DWSL consists of a number of GaAs quantum wells having two different thicknesses placed at random, with the additional constraint that one of them always appears in pairs (dimer well). Roughly speaking, resonances at specific energies arise due to the occurrence of paired wells and, most importantly, these resonances survive even if dimer wells are randomly distributed. Few years later, suppression of localization by correlations was further put forward for the explanation of the observed transport properties of GaAs/$Al_xGa_{1-x}As$ DWSLs [5].

Mainly, the suppression of electron localization in such systems is induced by tunneling of electrons created by the typical structure of the dimer cell which competes with disorder. More recently experimentally observation of superdiffusive transport has been reported in random dimer barriers [6]. Therefore, it is expected that this tunneling of electrons appears relevant to induce challenging transport properties.

In the present work we consider an SL, where two $Al_xGa_{1-x}As$ barriers of different Al mole fractions are introduced at random in the SL with dimer barriers located at random, referred to as DBSL. Such a DBSL consists of a number of $Al_xGa_{1-x}As$ quantum barriers having two different heights placed at random, with the additional constraint that one of them always appears in pairs (dimer barriers). Using the transfer-matrix technique, we determine numerically the miniband structure for both ordered, disordered and short range correlated SL by calculating the transmission coefficient.

2 Formalism

The one-electron effective-mass Hamiltonian of an electron moving in the potential of DBSLs is given by

$$\Big[-\frac{\hbar^2}{2}\,\frac{d}{dz}\,\frac{1}{m(z)}\,\frac{d}{dz} + V_{\text{SL}}(z)\Big]\psi(z) = E\psi(z)\,. \tag{1}$$

Here the SL potential V_{SL} derives directly from the different energies of the conduction band edge of the two semiconductor materials; namely GaAs and $Al_xGa_{1-x}As$ at the abrupt interfaces. Electronic states close to the conduction-band edge with vanishing momentum parallel to the layers are successfully described by the envelope function approximation [7]. In the following model, we consider that the height of the barriers takes at random only two values, namely V_a and V_b. These two energies are proportional to the two possible values of the Al fraction in the $Al_xGa_{1-x}As$ barriers, x, for $x \leq 0.45$. The sequence of energies is short-range correlated since V_b only appears forming pairs. At the

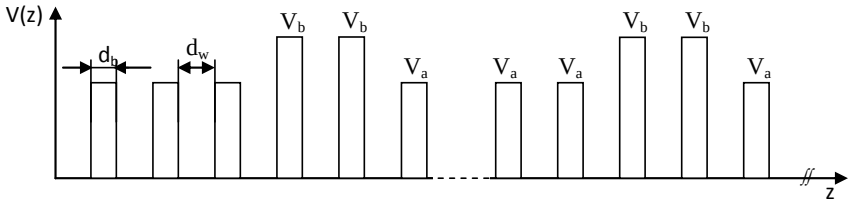

Figure 1. Schematic view of the conduction band-edge profile of the DBSL.

contacts of the DBSL sample the envelope function takes the form

$$\chi(z) = e^{ikz} + r_{_N} e^{-ikz} \qquad \text{for} \quad z < z_1 - d_b/2 \tag{2a}$$

$$\chi(z) = t_{_N} e^{ikz} \qquad \text{for} \quad z > z_{_N} + d_b/2 \tag{2b}$$

In Figure 1, we have depicted the conduction ban-edge profile of the DBSL, where pairs of V_b barriers appear at random. Here z denotes the coordinate along the growth direction of the centre of the n-th barrier, with

$$k = \frac{\sqrt{2m_w E}}{\hbar} \ . \tag{3}$$

Using Bastard's continuity conditions [7], the knowledge of the 2×2 transfer matrix $M(N)$ of the DBSL enables one to relate $t_{_N}$ and $r_{_N}$ in a closed expression. Defining

$$A_{_N} = \frac{1}{t_{_N}} \qquad \text{and} \qquad B_{_N} = \frac{r_{_N}}{t_N} \tag{4}$$

yields

$$M(N) \equiv \prod_{n=N}^{1} p_n \equiv \begin{pmatrix} A_{_N} & B_{_N} \\ B_{_N} & A_{_N} \end{pmatrix} \tag{5}$$

The SL can be viewed as an array of building blocks, each of them formed by an $\mathrm{Al}_x\mathrm{Ga}_{1-x}\mathrm{As}$ layer along with the two adjacent GaAs half-layers.

The transfer-matrix enables one to relate the transmission and reflection amplitude in a closed form. In the same manner for DBSL, the relationship between the reflected amplitude and the transmitted amplitude is given by

$$\begin{pmatrix} 1 \\ R \end{pmatrix} = M \begin{pmatrix} \tau \\ 0 \end{pmatrix} \ , \tag{6}$$

where

$$M = -\frac{m_w}{2ik} \begin{pmatrix} -\dfrac{ik}{m_w} & -1 \\ -\dfrac{ik}{m_w} & 1 \end{pmatrix} S(0,L) \begin{pmatrix} 1 & 1 \\ \dfrac{ik}{m_w} & -\dfrac{ik}{m_w} \end{pmatrix} \ . \tag{7}$$

Two values are allowed, corresponding to barrier height V_a and V_b, respectively. By taking into account the variation of the effective mass with respect to the Al mole fraction x, the effective mass in the n-th barrier can take two values m_a and m_b corresponding to barrier heights V_a and V_b, respectively.

The transmission coefficient is obtained from the ratio of the reflected and transmitted flow by

$$T = \tau ? \tau \,, \tag{8}$$

where

$$\tau = adfrac1M_{11} \,. \tag{9}$$

3 Results and Discussion

For a proper understanding, we have treated the above quoted GaAs/$Al_xGa_{1-x}As$ as semiconductor SL. The fundamental variable in our treatment is the Al concentration x which fixes both effective mass and height of the potential barrier V_{SL} within each layer of the structure. In particular, the SL potential may be expressed using the rule 60% for the conduction-band offset, via the relation

$$V_{\text{SL}} = 0.6 \times 1.247x, \qquad 0 \leq xeq0.45 \,. \tag{10}$$

This range of x ensures that $Al_xGa_{1-x}As$ presents a direct gap at the Γ valley. The effective mass in this region is given by

$$m(x) = (0.067 + 0.083x)m_0 \,, \tag{11}$$

m_0 being the free electron mass.

In the following numerical study, the electrons are assumed to propagate along the growing axis z. The choice is mainly motivated by the fact that all the parameters under consideration are experimentally realizable. Thus the present model serves as support for the observation of the Anderson localization. Typically a perfect binary alternating layers of GaAs and $Al_xGa_{1-x}As$ constituting a periodic array of barriers and wells of width $d_b = 25$ Åand $d_w = 100$ Å, respectively giving a period of $d = d_b + d_w$. The concentration of Al takes two values $x = 0.22$ and $x = 0.3$, which in turns yields two values for the heights of the barriers. For a band off set of 60% of the band conduction, the heights are given by

$$V_w = 0.06\Delta E_g = 190 \text{ meV} \qquad \text{for } x = 0.22 \tag{12}$$

and

$$V_b = 0.06\Delta E_g = 262 \text{ meV} \qquad \text{for } x = 0.3 \tag{13}$$

the band gap being related to the concentration via [8]

$$\Delta E_g = 0.1247x \,. \tag{14}$$

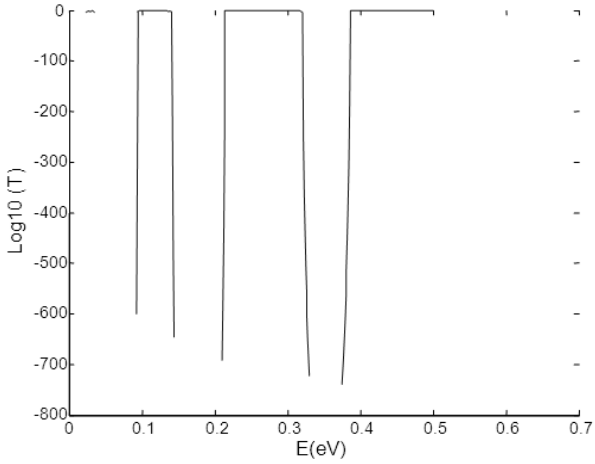

Figure 2. Logarithm of the transmission coefficient versus the energy for ordered case.

The number of periods has been fixed up to $N = 1000$ which provides a reasonable way in forming miniband structures.

The numerical calculations are reported for the results of the coefficient transmission versus energy in Figures 2–5 according to the above mentioned physical parameters.

For the ordered case, i.e. a perfect binary alloy material, which serves as reference, one can observe in Figure 2, the coefficient transmission versus the energy. Mainly it is shown perfect curves without fluctuations indicating clearly the existence of minibands separated by band gaps. Furthermore, the two minibands appear well defined with abrupt band edge as expected.

These two minibands exhibit very thin width lying within the well, the first varying from 20 to 30 meV, i.e. $\Delta E_1 = 10$ meV, and the second one from 92 to 144 meV, $\Delta E_2 = 52$ meV. The thin character of the minibands show clearly the ability of the chosen material GaAs/Al_xGa_{1-x}As with appropriate parameters in confining the electrons.

In the disordered case, the same structural parameters have been used for comparison. In the present context, the two kinds of barriers are distributed at random through the sample which provides a concrete illustration to the Anderson model, i.e. a disordered binary alloy.

In this disordered limit, as depicted in Figure 3, the first miniband disappears. Only the second one survives within the well starting from $E_{b_1} = 110$ meV up to $E_{b_2} = 140$ meV, i.e. the band width is about $\Delta E = 30$ meV. Here despite the one dimensional character of the sample under consideration, the Mott and Twose theorem implying the localization of all the electronic states for

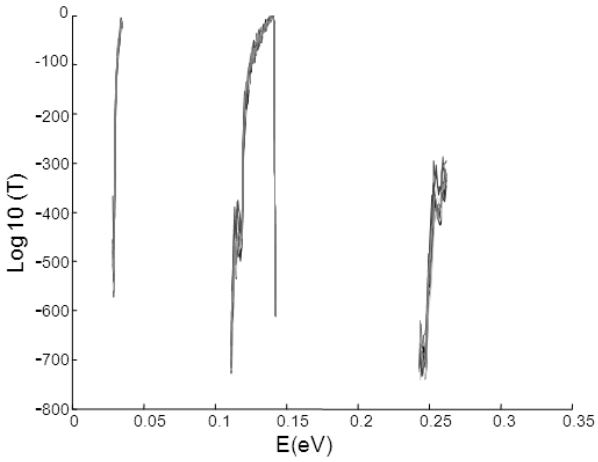

Figure 3. Logarithm of the transmission coefficient versus the energy for the disordered case.

any amount of disorder does not hold. First of all, we are dealing with a finite system while the theorem applies for an infinite one.

On the other hand, the periodicity of the one-dimensional lattice preserves the symmetry of the structure into the system leading to the possibility in creating constructive interferences and thus allowing the existence of minibands. Moreover, the minibands exhibits a tailoring band tail. The effects of the sample

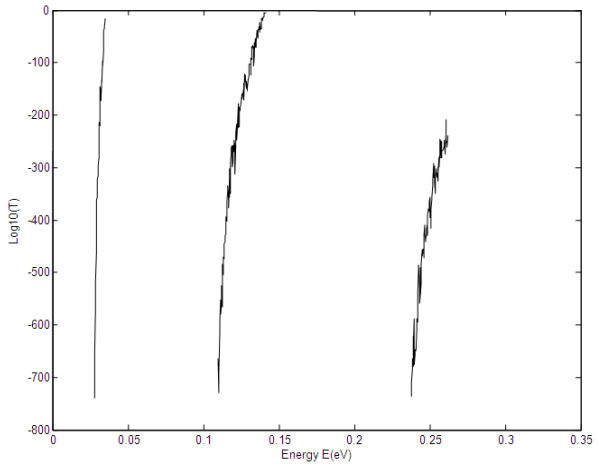

Figure 4. Logarithm of the transmission coefficient versus the energy for the disordered case with 10000 barriers.

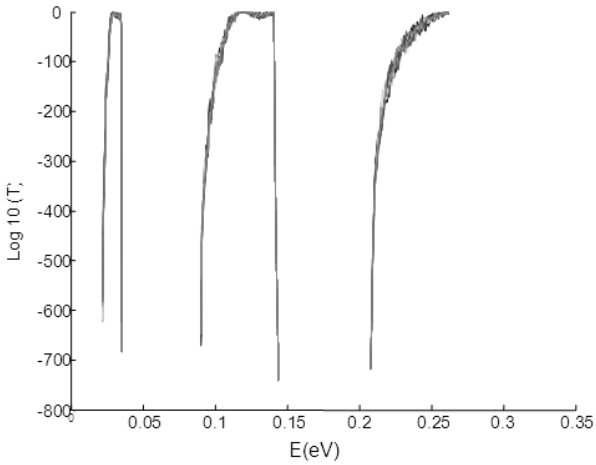

Figure 5. Logarithm of the transmission coefficient versus the energy for the correlated case.

size onto the localization have examined by varying the number of barriers from $N = 100$ to $N = 10000$. It is clearly shown in Figure 4 that the electronic localization is more efficient for larger sample.

However the effects of disorder on the structure of the miniband are noticeable. One can observe the strong asymmetric character of the miniband (see Figures 3 and 4). The upper band edge appears abrupt while the transmission coefficient exhibits a decrease at lower energies over a range ΔE for the second miniband. Thus the disappearance of the first miniband and the asymmetry of the second one are a signature of disorder inducing localization. Moreover it is clearly shown the ability of disorder in destroying the lower electronic states, i.e. the more confined states.

In presence of random dimer, i.e. the appearance of paring cell with a concentration of 10% introduced into the material, the over whole structure of the two minibands is well preserved. However some significant changes occurs. In the presence of correlation in disorder as reported in Figure 5, one can observe the existence of two minibands having exhibiting well defined structures. Only a minor asymmetric aspect is revealed. Moreover, the widths of the minibands are weaker than the ordered case, $E_{b_1} = 52.4$ meV and $E_{b_2} = 104.8$ meV. This feature translates the effects of disorder. Surprisingly, the minibands are lower in energies. This statement is mainly due to the correlation in disorder which restores the tunnel effect. This later acts significantly in confining the electronic states. Obviously, this aspect may be greatly appreciated for technological purposes. It could be also noticed that all these effects are not qualitatively sensitive to the amount of the concentration of dimer. The variation of the concentration

changes only the fluctuations observed in the coefficient transmission close to its maximum. Moreover it could be observed that the transmission coefficient versus the energy takes very high magnitude, T close to unity, leading to very large efficiency for electronic transport which gives some bearing to the notion of superdiffuse transport as reported experimentally [6].

In conclusion, from the fundamental point of view, the present numerical study yields a proper understanding of the transition from localized to delocalized states from the order limit is achieved.

References

[1] P.W. Anderson (1981) *Phys. Rev. B* **23** 4828.

[2] E. Diez, A. Sanchez, F. Domınguez-Adame (1994) *Phys. Rev. B* **50** 14359; F. Domınguez-Adame, A. Sanchez, E. Diez (1994) *Phys. Rev. B* **50** 17736.

[3] N.F. Mott and W.D. Twose (1961) *Adv. Phys*. **10** 107.

[4] E. Diez, A. Sachez, F. Domınguez-Adame (1995) *IEEE J. Quantum Electron*. **31** 1919; E. Diez, A. Sachez, F. Domınguez-Adame, G.P. Berman)1996) *Phys. Rev. B* **54** 14550.

[5] V. Bellani, E. Diez, R. Hey, L. Toni, L. Tarricone, G.B. Parravicini, F. Domınguez-Adame, R. Gomez-Alcala (1999) *Phys. Rev. Lett.* **82** 2159.

[6] U. Naether, S. Stüzer, R.A. Vicencio, M.I. Molina, A. Tünnermann, S. Nolte, T. Kottos, D.N. Christoodoulides, A. Szameit (2013) *New J. Phys.* **15** 013045.

[7] G. Bastard (1989) "*Wave Mechanics Applied to Semiconductor Heterostructures* (Editions de Physique, Paris).

[8] S. Adachi (1985) *J. Appl. Phys*. bf58 R1.

[9] G. Bastard (1981) *Phys. Rev. B* **24** 5693.